SSC Detector Subsystem R&D Proposal to Develop Track and Vertex Detector Based on Silicon Drift Devices.

W. Chen, H. Kraner, Z. Li, H. Ma, V. Radeka, P. Rehak, S. Rescia
Brookhaven National Laboratory, Upton NY 11973

J. Clark, J. Oliver, R. Wilson
Harvard University, Cambridge, MA 02138

T. Humanic, D. Kraus, T. Smith, B. Yu
University of Pittsburgh, Pittsburgh, PA 15260

K. McDonald, C. Lu
Princeton University, Princeton, NJ 08544

A. Vacchi
Rockefeller University, New York, NY 10021

G. Bertuccio, E. Gatti, A. Longoni, M. Sampietro
Politecnico di Milano, Piazza Leonardo da Vinci 32, Milano

P. Holl, L. Strüder
Max-Planck-Institut for Extraterrestrial Physics, D–8046 Garching

E. Lorenz
Max-Planck-Institut for Physics, D–8000 Munich 40

U. Faschingbauer, A. Wörner, P. Wurm
Max-Planck-Institut for Nuclear Physics, D–6900 Heidelberg 1

J. Kemmer
Technische Universität München, D–8046 Garching

ABSTRACT

We propose to develop a vertex and an inner tracking detector for the SSC based on Semiconductor Drift (Memory) Detectors. We believe that silicon drift detectors are ideal detector elements to be used for the charged particle tracking close to the interaction region of the SSC for the following reasons:

1. the unambiguous position resolution of only several μm in two perpendicular directions
2. attribution of hits belonging to different bunch crossings with a timing accuracy better than $1ns$ and
3. the intrinsic signal pipeline within the very volume of the silicon drift detector.

The inner tracking detector extends radially at most to about $50cm$ from the beam axis. We assume larger gas detectors follow behind the inner tracking detector. Only the inner tracking detector and the vertex detector are the topics of this proposal.

1. Introduction

We propose to develop a high resolution charged particle tracking and vertexing subsystem to solve the challenge of particle tracking at small distances from an interaction region at the SSC. The system is based on silicon drift detectors – relatively new but well tested devices. We propose the following steps leading to the development of the complete system:

1. To design silicon drift detectors "matched" to the SSC environment, that is, particle rates and a very likely presence of a strong magnetic field around an intersection region. The silicon drift detectors must have a drift speed calibration system to eliminate the need for a precise monitoring of the detector temperature.

2. To develop low noise fast preamplifiers integrated on the silicon wafer of the detector with acceptably low power dissipation.
3. To produce desirable silicon drift detectors with integrated preamplifiers on the same wafer.
4. To test the performance of silicon drift detectors and the integrated electronics with the emphasis on the system stability and reliability.
5. To test the radiation damage and the high temperature annealing of silicon drift detectors with integrated electronics.
6. To design a complete read-out system of silicon drift detectors for the SSC application.
7. To study and to develop a fast trigger from silicon drift detectors.
8. To design the tracking and vertexing system, to build at least one sector of it and to test its performance at a high energy test beam.
9. To study the performance of the system at the "SSC environment" with the Monte Carlo method. We plan to use the test beam results and Standard Model Higgs production mechanism and decays to evaluate and to improve the performance of the tracking system. To test the vertexing system we plan to Monte Carlo B decays in the central region.
10. To study and to develop a read-out system which is mostly blind to hits due to spiraling low momentum tracks.

The second section will summarize principles of silicon drift detectors. It will explain why a pair of silicon drift detectors can determine the time of the particle crossing with the precision better than $1ns$ and why the detector itself is the first signal pipeline in the read-out system. The third section will present the general concept of a silicon drift detector based tracking and vertexing system. In the fourth section we will elaborate all

tasks of the proposal and assign responsibilities for each task. In the fifth section we will define our milestones and we will conclude with the budget estimate.

2. Semiconductor Drift Detectors

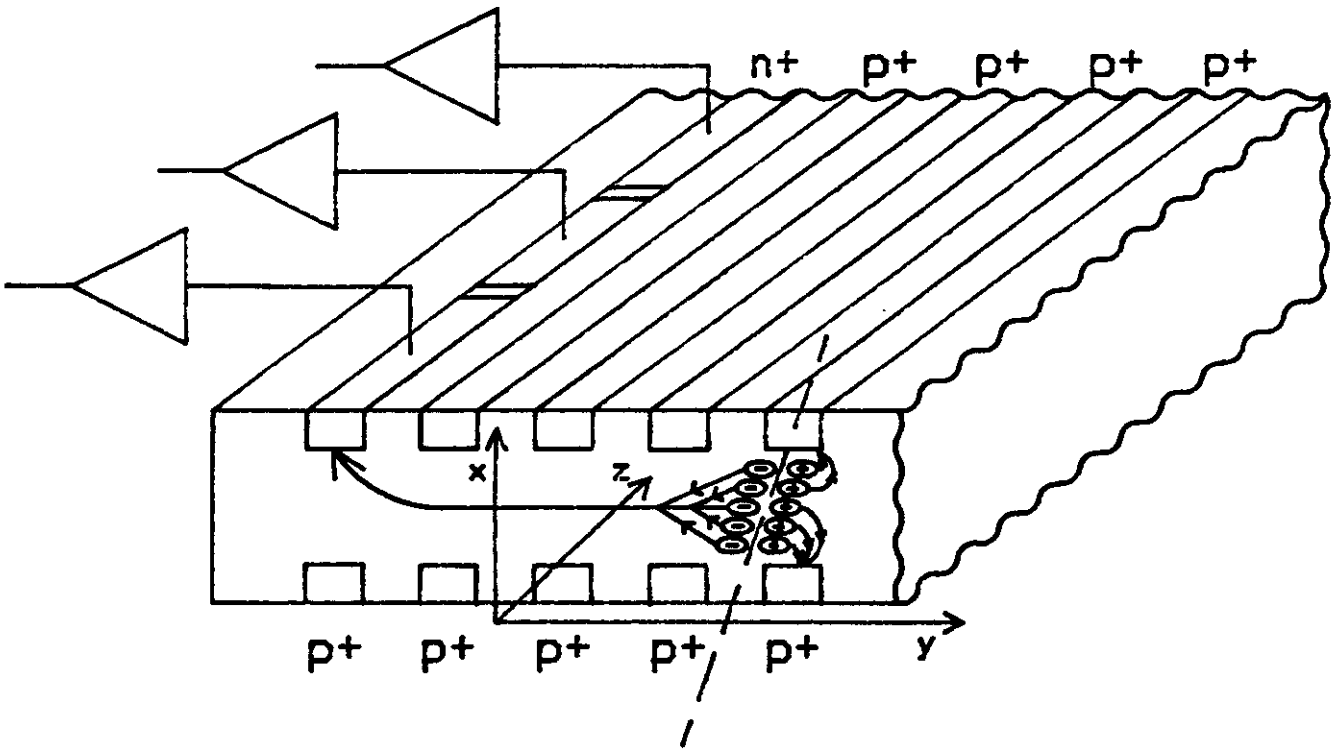

Figure 2.1: Perspective view (not to scale) of a semiconductor drift detector. Electrons created by an ionizing particle are transported long distances parallel to the detector surface. The anode is divided into short segments to measure the coordinate perpendicular to the drift direction.

Silicon drift detectors are relatively new kind of semiconductor detectors able to provide very precise position and ionization measurements with a very modest amount of electronics. A perspective view of the drift detector[1] is shown in Fig. 2.1. In principle, the electric field of the drift detector forces electrons liberated by an ionizing particle to drift parallel to the large semiconductor surface to the anode. The transit time of electrons

inside the detector measures the distance of an incident particle from the anode.

As a direct consequence of this electron transport method the anode capacitance is much lower than the anode capacitance of the classical semiconductor detector of the same dimensions. The amplifier noise can be made much smaller which is the main reason behind the excellent position resolution of silicon drift detectors.

The measured position resolution in a test beam was $10\mu m$ on the drift distance of $4000\mu m$. These results[2] were achieved with external amplifiers which were not matched to the very low anode capacitance.

As an example, the drift detector to be used in UA6 experiment at CERN SPPS has an area of $4cm \times 4cm$, maximum drift time of $1.5\mu s$, total number of anodes 332 and an unambiguous x-y position resolution of $10\mu m$ in both directions.

We would like to stress that the maximum drift time is not the dead time of the silicon drift detector. Due to the fact that all electrons are continuously drained at the anode the silicon drift detectors have no dead time. Electrons drifting toward the anode have their charges screened by the electrode structure of the silicon drift detector and do not interfere with the other signals or with the signal processing at the anode. The signals are stored within the detector for the duration of their drift. In the high rate environment of the SSC a silicon drift detector stores at any given time hits of particles originated at different bunch crossings.

Fig. 2.2 shows a simple way how to resolve particles originated at different bunch crossings. Two silicon drift detectors are placed parallel one to another at a small distance.The drift fields in the two detectors are arranged in such a way that electrons drift in opposite directions in these two detectors. Following some easy calculations in Fig. 2.2 we see that there is a constraint for the sum of the drift times measured in both detectors with respect to the time of the particle crossing. The time resolution of each drift detector is better than $1ns$. The mean value of the drift times of the

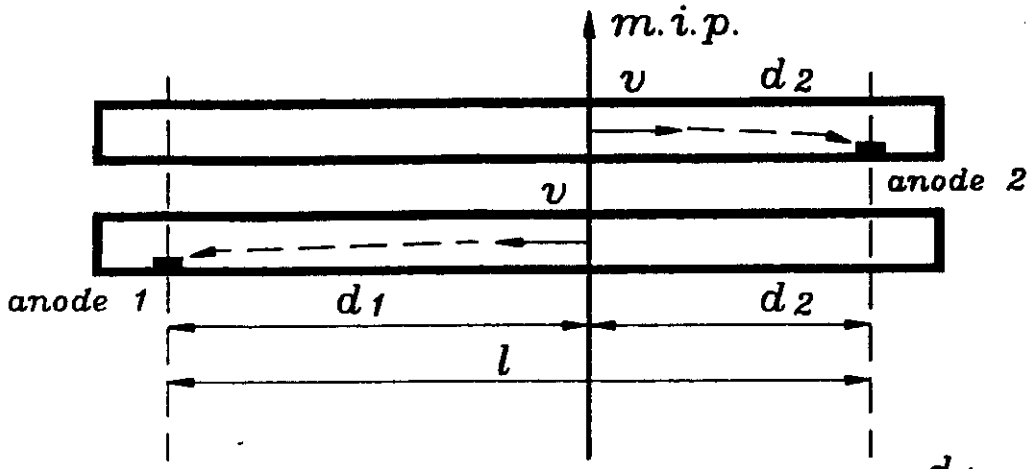

$$d_1 + d_2 = l \qquad t_1 = t_{bunch} + \frac{d_1}{v}$$

$$\frac{t_1 + t_2}{2} = t_{bunch} + \frac{l}{2v} \qquad t_2 = t_{bunch} + \frac{d_2}{v}$$

Figure 2.2: View (not to scale) of two silicon drift detectors placed in such a way that a particle has to cross both detectors and the produced electrons are drifting in opposite directions with the same speed v. The sum of drift distances for any position of the incident particle is constant and equals to the distance between anode1 and anode2. The average of two arrival times gives the time of the bunch crossing.

pair of drift detectors and hence the bunch crossing timing can be determined with the resolution better than $1ns$. There are not many position sensing detectors with this kind of time resolution.

We should now stress that there is no penalty to pay by using two silicon drift detectors instead of one. Once the association of hits with bunch crossing is completed we have two independent measures of points leading to a vector. This "vector" geometry is most likely preferable also

from the pattern recognition point of view. Later we will see that our conclusions are correct even in a case of silicon drift detectors inside a magnetic field.

Equations in Fig. 2.2 are strictly speaking valid only for a given angle of incidence or for a zero distance between the two detectors. If we assume $1.5mm$ distance between the two silicon drift detectors and the drift speed of $20\mu m/ns$ accepted angular spread is $2 \times 20\mu m/ns \times 8ns/1500\mu m \approx 0.2rad$. The larger angular spread can be recognized in the reconstruction and all hits correctly associated. We can even think about a set–up of several layers of silicon drift detectors with the drift direction reversed from layer to layer but without being in close pairs to provide the full bunch crossing association after an offline global fit to the track candidate.

The total memory time is about $1.0\mu s$ for $2cm$ of drift path. Due to the very high "virtual" segmentation of the detector the degree of confusion from too many hits at one anode of the detector is negligible. The optimal drift length can be chosen according to the location of the detector in the experiment.

In this proposal we will consider two kinds of silicon drift detectors. Silicon drift detectors with a linear anode and with pad anodes. In a linear silicon drift detector there is only one (or only a very few) strip–like anodes. The drift time measures one coordinate very accurately; the other coordinate is within the length of the linear anode. The position information provided by a linear silicon drift detector is of the same kind as silicon microstrip detector but the number of read–out channels is about three orders of magnitude reduced.

Fig. 2.1 shows the collection anode divided into individual pad–anodes. The position of the responding anode(s) measures the coordinate perpendicular to the drift direction. Due to the transverse diffusion, the electrons produced by the ionization arrive as a gaussian shaped charge cloud in the anode region. Charge will be usually collected on more than one anode. The charge division method yields the position of the crossing particle in

the second coordinate with a precision down to about 4% of the anode–pad pitch. This multi–anode silicon drift detector provides an unambiguous two dimensional position information. The position information is similar to one which is to be expected from proposed silicon pixel devices. The multi–anode silicon drift detector gives better resolution with four orders of magnitude less read–out channels.

Silicon detectors are capable of achieving the position resolution of $4\mu m$ with a detector $300\mu m$ thick. These best result were obtained with a normal incidence of charged particles. For other angles of incidence the resolution will be limited by the fluctuations in the density of the ionization (Landau) in the silicon. For an inclined incident angle the best position information which can be obtained from any silicon detector is the center of gravity of the ionization. This information on average is the crossing of the particle trajectory with the middle plane of the detector. Due to the fluctuations in the linear density of the ionization the charge center of gravity fluctuates. A detailed analysis is on Page 370 of Ref. 2 and shows that for a non normal incidence there is an additional contribution to the position resolution due to the fluctuations in the ionization density $\sigma_l = t \times tan(\alpha) \times \sigma_Q/Q$ where t is the thickness of the detector, α is the angle of the incidence and σ_Q/Q is the relative width of the Landau fluctuations in the silicon of the thickness t (≈ 0.2 for a $300\mu m$ thick silicon).

Presence of the magnetic field modifies trajectories of electrons in a silicon drift detector and a normal incidence is not more the ideal one. There is,however, a proper incidence angle which does not produce any degradation of the position resolution. We will keep this in mind in the next section while designing the inner tracking detector.

3. Tracking and Vertex Detector Lay–out

Fig. 3.1 shows the axonometric view of the Inner Tracking Detector. The bottom part of Fig. 3.1 shows the same view with a cut in front part

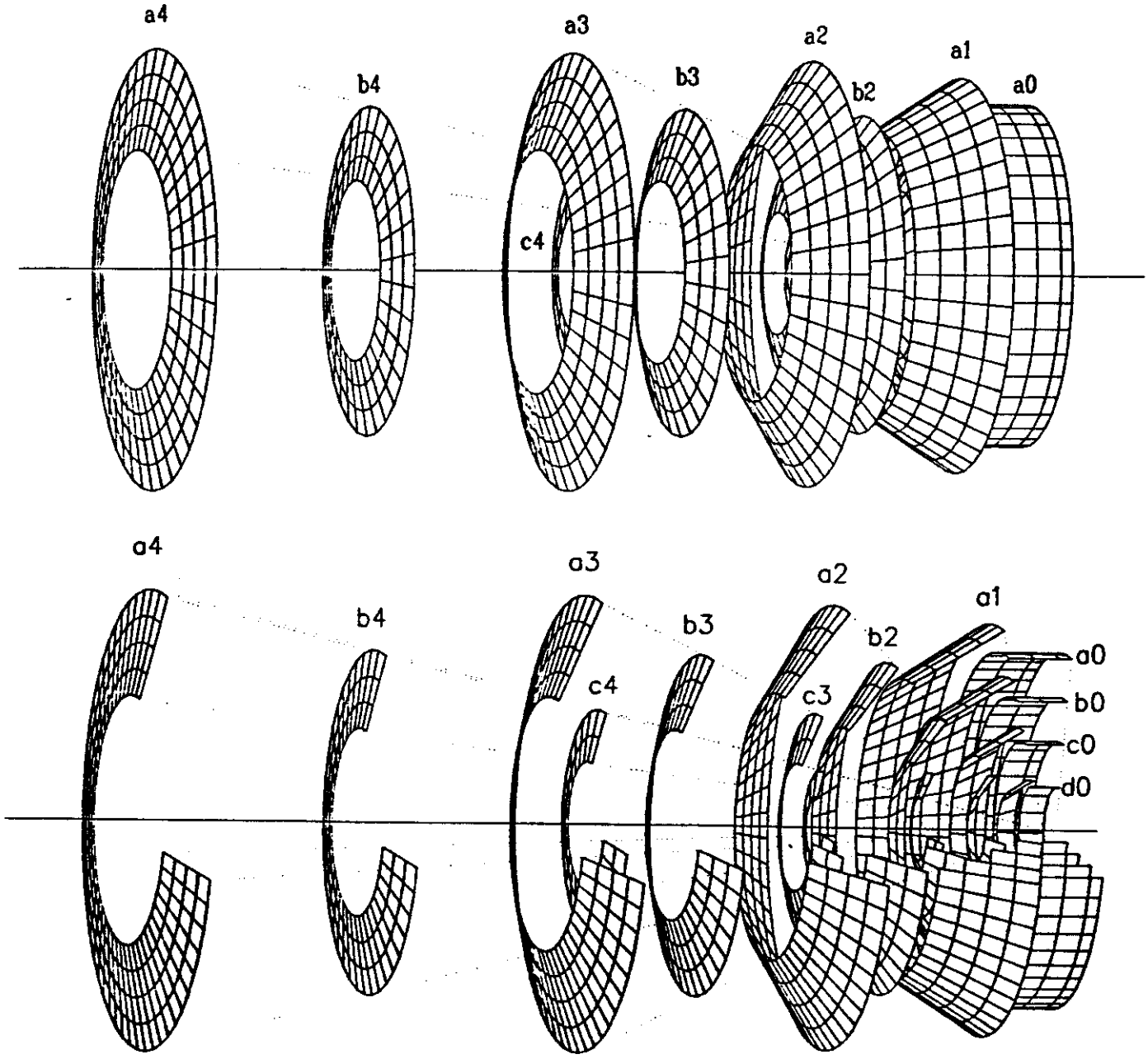

Figure 3.1: Axonometric view of the left half array of silicon drift detectors forming the inner tracking detector. Each ring consists of two layers of silicon drift detectors to provide the correct association with the bunch crossing and to provide a "vector" information. In the bottom view the front angle of each ring is cut off to show hidden rings.

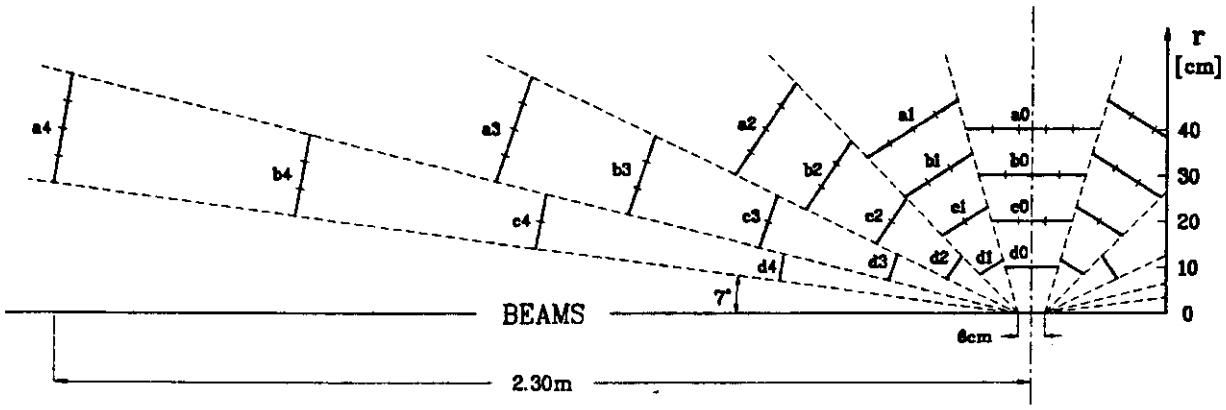

Figure 3.2: Cross section along the beam axis of the inner tracking detector based on silicon drift detectors. Detector has a full azimuthal coverage and rapidity coverage $|\eta| \leq 3$. Lines indicate the cross section of rings of detectors centered around the beam axis. Each line represents close layers of silicon drift detectors.

of rings to show the hidden complexity close to the interaction region. Now we will define this detector geometry and we will justify our choices.

Fig. 3.2 shows the cross section of the tracking detector along the beam axis. We will assume a uniform magnetic field along the beam direction (solenoidal field). We can see different sectors and different layers in Fig. 3.2. Sectors are called $0, 1, ..., 5$ and each sector covers a certain region in rapidity. Layers have letters a, b, c and d and are placed roughly at $40, 30, 20$ and $10cm$ from the beam. The most important requirement is the perpendicular incidence of fast particles onto the detector surface. There is only a very small overlap between the neighbouring sectors. The position of the individual sectors along the beam direction is defined by this non overlaping requirement, normal incidence and by the average distance from the beam axis which is kept constant for all sectors.

The proposed geometry is a good compromise between the size of the detector in the forward direction and the increase of the density of the

particles toward higher values of the rapidity η. The geometry minimizes the amount of silicon to cover given solid angle at any distance. Last but not least the silicon drift detectors in this geometry are less likely to be crossed by low energy spiraling tracks.

The shown geometry of the tracking detector takes a full advantage of the relatively small size of individual silicon drift detectors which is usually considered a general shortcoming of all silicon detectors. The size of individual silicon tiles is about $6.5cm$ because we have assumed that silicon drift detectors are made from 4 inch diameter wafers. There are no 4 inch diameter high resistivity detector grade silicon wafer available in 1989. The maximum diameter is 3 inch. We hope that 4 inch wafers will be commercially produced by 1992. The total number of wafers is about 8000 having the total active area of $20m^2$. Each fast particle is measured 8 times.

Fig. 3.3 shows the azimuthal view of the four double layers of the central sector (number 0) of the inner tracking detector. The magnetic field is assumed to be parallel to the beam direction, and in this view we see and measure the magnetic curvature. Drift of signal electrons within silicon drift detector is in the plane of the drawing and electrons are subject to Lorentz forces. A direct analysis of the electron transport in semiconductors in a magnetic field is a well known subject of solid state physics. The electron mobility becomes a tensor quantity with all components being functions of the magnetic field. Electron transport equations in a magnetic field have an analytical solution for the case of the electric field of the silicon drift detectors. We will give here only relevant results.

There is a substantial difference between the behaviour of silicon drift detectors and gas drift chambers in a magnetic field. In a gas chamber the electrons do not drift along the electric field lines and they spiral before reaching the anode wire. In a silicon drift detector placed relative to the magnetic field as shown in Fig. 3.3, electrons drift parallel to the large surfaces of the detector along the applied drift field. The magnetic force is

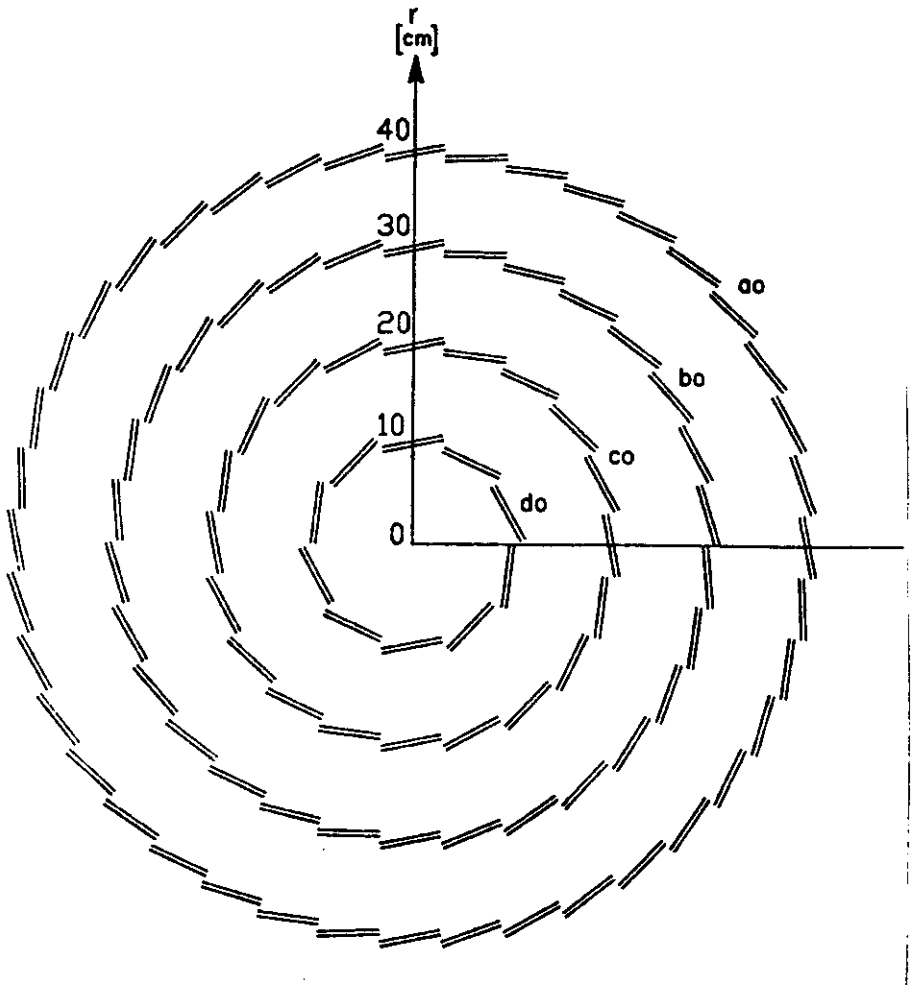

Figure 3.3: Cross section of the inner tracking detector perpendicular to the beam in the center of the interaction region. Magnetic field of $1.5T$ parallel to the beam direction is assumed. Detectors are tilted by 11° with respect to the azimuthal direction. The tilt corrects for the magnetic phenomena of the electron transport in silicon.

compensated by the confining electric field within the silicon drift detector. Instead of being transported in the detector midplane electrons are transported in a plane slightly shifted out of the plane of minimal potential energy. During the drift the Lorentz force is exactly compensated by the component of the electric force of the confining field. There is no change of the drift velocity or other adverse effects during the main signal transport as compared to the drift without the magnetic field.

Special care has to be taken during the very first instance of the detection process when the electrons are produced more or less uniformly across the detector and are moving toward the midplane due to the confining electric field of the silicon drift detector. There are Lorentz forces acting on electrons during their initial drift too. For a normal incidence the charge would form a line instead of a point in a drifting plane. Fig. 3.3 shows all silicon drift detectors in the central sector to be tilted with respect to the normal incidence. The tilt angle is exactly the Hall angle defined by the relation $tan(\alpha_h) = \mu \cdot B$ where μ is the electron mobility and B is the magnetic field.

It can be shown that if a charged particle crosses the detector in the direction inclined from the normal incidence by the Hall angle α_h all electrons produced by the ionization come together in a point in the drifting plane. The fluctuations of the ionization density thus do not degrade the position resolution of the silicon drift detector. Fig. 3.4 shows the trajectories of electrons in more detail and moreover shows that this isochronism is valid in both direction of the drift field. Two layers of silicon drift detectors can again associate the hit with the correct bunch crossing.

The silicon drift detectors of the sector number 4 are oriented almost perpendicular relative to the external magnetic field. (This orientation is not the best for the momentum analysis of the charged particles. There is little of the useful magnetic deflection. This is not due to the position of the detectors but due to the geometry of the solenoidal magnetic field.) In the asymptotic case of the magnetic field perpendicular to the surface of the silicon drift detector electrons drift in the middle plane of the detector, however, the direction of the drift is rotated by the Hall angle α_h with the respect to the direction of the drift field E_d. The drift speed is reduced by the factor of $\sqrt{1+(\mu \cdot B)^2}$. The isochronous lines remain normal to the detector surface as was the case of no magnetic field.

Silicon drift detectors have to operate under slightly higher drift field (2% increase for an external field of $1.5T$). The drift non parallel to the drift

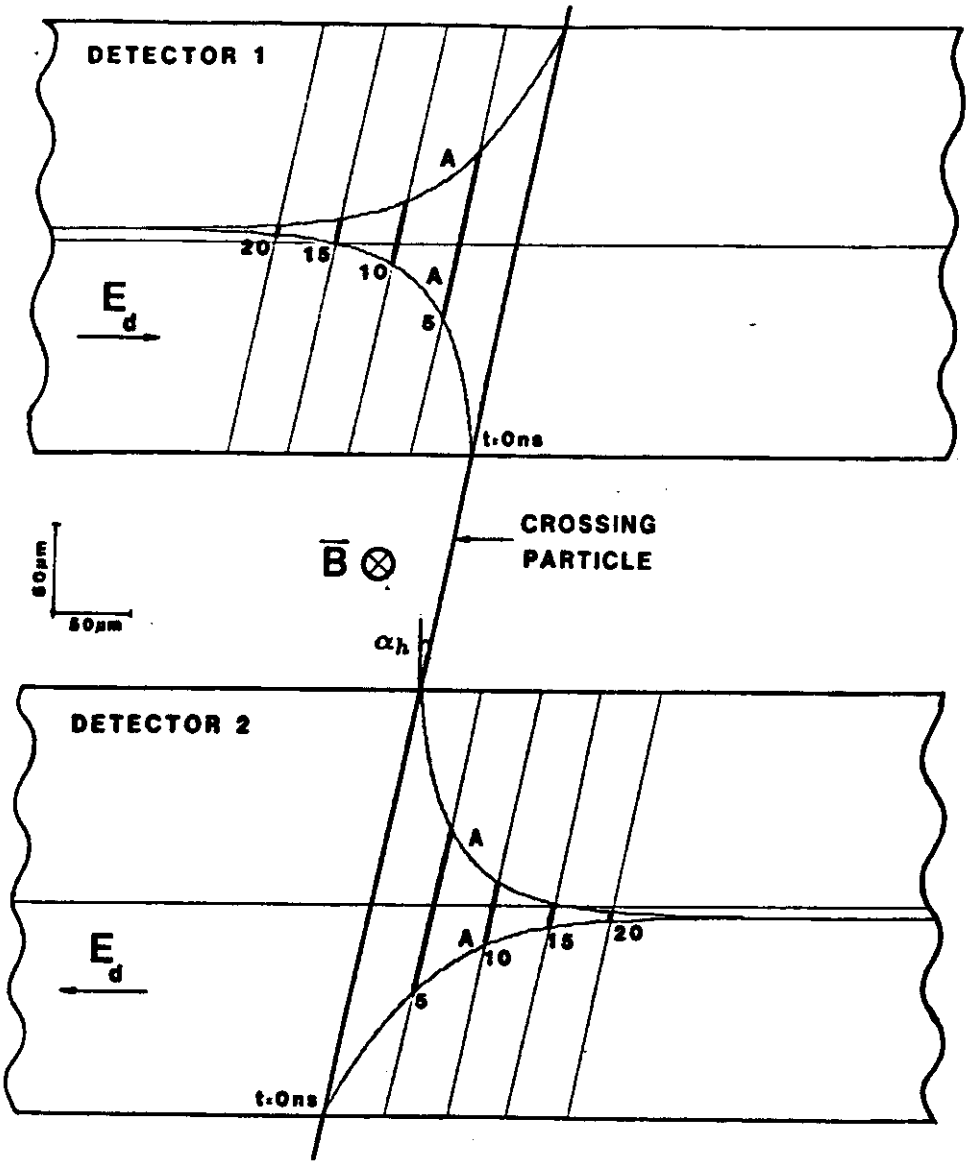

Figure 3.4: Trajectories of electrons ("A" in the Fig.) generated by an ionizing particle incident under the Hall angle α_h. Parallel lines define isochronous points on the trajectories. All electrons created by the ionization of the crossing particle are brought to a point independently of the direction of the applied drift field. Association of a hit is done in a same way as in a case without a magnetic field.

field can be compensated by rotation of individual silicon drift detectors or by taking the effect into account in software. The sectors number 1, 2 and 3 have magnetic field at an angle between 0 and 90^o relative to the detector orientation. These sectors are tilted in the azimuthal direction by an angle smaller than the tilt of the central sector. They also have the above mentioned increase of the drift field.

We do not insist on the finality of the presented design of the inner tracking detector. Within this proposal we are indeed planning to evaluate it and to improve it. We believe strongly, however, in the basic concept of the present design. The basic features of the design are given by the physics of the p–p interactions and by the physics of the particle detection in the silicon drift detectors. The magnetic field influences the design only in a second order defining the tilt angles and a slight increase of the drift field. Thus our design of the inner tracking detector looks essentially same in the case, let us say, of a dipole field or of a non magnetic detector.

We have not mentioned the vertex detector up to now. There is no sharp boundary between the vertex and the inner tracking detector. We can think of layer *d* as being the last layer of the vertex detector. Two additional double layers *e* and *f* can be added closer to the intersection region. They are made with smaller wafers to approximate better a normal or "tilted" incidence. (We may already use smaller detectors for the layer *d* for the same reason.) The exact location and the geometry of the layers *e* and *f* will be one of the tasks of this proposal. The distance and the geometry depend very critically on the required physics goals and on the exact size of the intersection diamond. It may be that for heavy flavor physics an intersection region with much shorter diamond length is preferable in spite of the consequent decrease of the luminosity.

We did not specify where there is going to be transition from multi–anode silicon drift detectors to linear anode detectors. We will decide the question in point 9 of the proposal task.

The very important subjects of heat dissipation, cooling, radiation damage and complete read out system will be addressed in the next section.

4. Proposal Tasks

The division of the work into ten different tasks is rather arbitrary and all tasks are closely interdependent. We will mention nevertheless institutions mostly responsible for the given tasks in spite of the fact that in past all persons in the group collaborated very closely together with no institutional boundaries. The three different institutions in Munich and Garching will be referred to just as one institution.

4.1 Design of silicon drift detectors

Institutions: BNL, Milano, Munich

Proposed devices are well tested silicon drift detectors. For a SSC application we have to pay more attention to the following features:

1. Radiation hardness
2. Cooling of detectors with integrated electronics
3. Reliable position calibration in both directions

1) Silicon drift detectors do not have any useful MOS structure, therefore are as radiation hard as the silicon bulk devices. Moreover, we have designed, produced and successfully tested a silicon drift detector[8] where all current generated on $Si - SiO_2$ interface is collected by a sink anode instead contributing into the leakage current of the signal anode. Presently (September 1989) we have finished the design of a $32cm^2$ large silicon drift detector for the CERN experiment NA45 which also collects the interface generated current into a sink anode. With this design any radiation damage of the interface would not degrade the performance of the silicon drift detector. Radiation damage of the interface is very pronounced in strip and pixel detectors

Bulk damage of silicon drift detectors may already be a problem at the SSC environment if some accidental beam loss during filling periods

is taken into account. We propose to design the supporting system with all connections in such a way that each silicon drift detector can be fast disconnected from the main support and thermally annealed. We have developed this kind of support for the silicon drift detector to be used in the NA45 experiment. The "fast disconnect" was realized by one dimensional rubber contacts developed for the watch industry.

2) The voltage divider alone dissipates about $200mW$ of power per a single silicon drift detector of the area about $40cm^2$. For the complete inner track detector the total power would be up to $2kW$. It is not too hard to take this power out. However, silicon drift detectors are very temperature sensitive and special care is needed when cooling the detectors. There is one important point with the power dissipation. We have a full control to decide where the integrated voltage divider is located on the silicon drift detector, that is, where the heat is generated. The same is true to some extent for the location of the integrated electronics. For the SSC design we have to place all heat sources close to the edge of the detector where the heat is going to be taken away without flowing through the silicon. The design of the external cooling system is a part of the task number 8.

3) The calibration is closely related to the temperature stability. The drift velocity in silicon is proportional to the drift field $v_{drift} = \mu \cdot E$, where μ is the electron mobility ($1400cm^2/Vs$). The mobility and therefore also the drift velocity are temperature dependent $\mu \sim T^{-2.4}$. Due to the precision of silicon drift detector we are sensitive to temperature variations of about $0.1K$. Furthermore the temperature must be uniform in the sensitive volume of a drift detector.

Stabilizing the overall temperature to better than $0.1K$ may not be practical. It seems easier to calibrate the drift velocity. We consider to implement two calibration systems.

a) calibration by electronically injected electrons at a well defined position in a silicon drift detector. Electrons can be injected directly from

an ohmic contact or from a local potential minimum where thermally generated electrons are stored and eventually released by an external trigger. Both types of injectors are currently under study.

b) Laser light calibration. Optical light can be focused on a silicon detector yielding a well defined spot, but all the photo–ionization occurs very near the surface and does not simulate effects of the ionization by a charged particle. Silicon is almost transparent to infrared photons of energy also slightly above the $1.1eV$ band gap. By a fortunate coincidence the photon energy of a Nd:YAG laser is $1.16eV$, and the absorption length in silicon is $1mm$. This light can be used not only for the monitoring of the drift velocity but also for the calibration of the relative positions of different layers.

4.2 Integrated preamplifiers

Institutions: BNL, Milano, Munich

This task is already partially funded from the other SSC generic R&D detector development grants. The low noise fast preamplifier on high resistivity silicon of the detector grade wafer was designed,[4] produced and tested[5]. In spite of unwanted parasitic connections between power busses the whole preamplifier works[6]. Design is based in a new type of JFET and is intrinsically radiation hard. The power dissipation of a single preamplifier is about $5mW$. We plan to develop a bipolar transistor for the output driving stage which will bring the power dissipation down to $1mW$ level. We think the problem is well under control as can be seen from [4-6] .

4.3 Production of silicon drift detectors

Institutions: Munich

4.4 Lab test of performance

Institutions: Pittsburg, Princeton, Rockefeller

A series of long time test will be performed in labs with the ionization simulated by the infrared light. We will use partially existing lab equipment. (Micropositioners, Microscopes etc.)

4.5 Radiation damage

Institutions: BNL, Heidelberg

We have mentioned earlier the intrinsic radiation hardness of silicon drift detectors. Due to the importance of the problem in the SSC environment we will elaborate the radiation tests into some detail.

In order to fully exploit the silicon drift chamber as a tracking device for the SSC, one must consider possible radiation effects and ask if enough is known to predict the effect on silicon drift detectors. Several workshops have been held by the SSC Central Design Group to consider

1. the radiation environment within the colliding region and
2. the effect of this environment on materials and detectors.

These findings have been published as SSC-SR-1033 and SSC-SR-1035 respectively and we can expect two major components to the annual radiation dose:

1. 2.4×10^{12}, $1MeV$ fast $neutrons/cm^2$ as albedo from the calorimeter
2. $1MRad$ due to charged particles (mostly minimum ionizing) which approaches $10^{14}/cm^2$ in fluence, at distances $8cm$ from the beam axis.

These numbers result from the assumption that the central cavity around the collision region is $2m$ and that a heavy calorimeter is in place. Other radiations such as an albedo photon flux will not be important to the detector, but may have an effect on the readout electronics. While there is some latitude in hardening the electronics, charged particles and neutrons will cause volume displacement effects that are not amenable to cures, other than annealing.

Fast neutrons and charged particles cause displacement of silicon atoms from their lattice sites which results in both, generation centers and trapping centers. Other effects such as majority carrier removal and surface

effects will need not to be considered. The increase of leakage current from generation centers is well recorded and well-studied at this time[7].

Trapping effects are often neglected when evaluating simple charge collection across a $300\mu m$ wafer associated with a Landau distribution of energy loss, however we must consider trapping is the case of drift events having electron trajectories of up to $1cm$. Deep traps generally hold charges for times greater than the collection time in most detectors: Thus, in a drift detector, some trapping of the mobile electrons will simply reduce the charge signal, but have little influence on the timing and position determination. It is possible, but unlikely, that a trapping/detrapping combination could act to obscure the time centroid of the collected charge packet.

In other materials as well as silicon, hole trapping is predominant from fast neutron-induced cluster displacement damage. Fortunately, holes are quickly collected and do not contribute to the signal formation. Electrons form the charge packet may be less susceptible to trapping. Very few estimates of electron trapping in silicon seem to exist in the literature, except for some results dating to 1968 and 1971. Coleman et al.[8] and Liu and Coleman[9] irradiated totally depleted thin surface barrier transmission detectors with protons between 0.8 and $5MeV$ to fluences to over 10^{15}. The n^+ and p^+ contacts of the detectors were scanned with an alpha source which elicited either hole or electron traversal of the detector. At fluences in the $10^{13}/cm^2$ range considerable hole trapping was indicated by degradation of the alpha peak with the source incident on the n^+ contact. Their data also indicate electron trapping for higher fluences of protons which traversed the entire detector although their interpretation of the data is not explicit in this regard. If one scales the effects between $4MeV$ protons and minimum ionizing radiation by a factor of 100, one might expect the trapping at a m.i.p. fluence of several times $10^{15}/cm^2$. However, it must be noted that their collection depth was only $100\mu m$. There is therefore a distinct possibility of performance degradation of drift detectors from electron trapping introduced by the SSC radiation environment.

Clearly, the extrapolation of older results for charged particle effects is somewhat tenuous and one must surely perform more pertinent measurements with representative structures. Further, these early measurements are strictly applicable to the charged particle component to the expected SSC annual dose. Measurements with fast neutrons should also be made on representative structures. At higher energies neutron damage tends to be more equivalent to proton damage as the silicon recoil becomes more energetic and the displacements (knock-ons) are more widely spaced and take on the character of isolated point defects. However, the neutron-proton distinction only becomes lessened at neutron energies above $14MeV$, whereas the expected SSC neutron fluence will be about $1MeV$. This point is made to caution the application of the proton results too widely. As opposed to minimum ionizing particles the proton-induced damage is more comparable to fast neutron damage, but it should not be strictly compared to $1MeV$ neutrons. Therefore, more applicable data should be acquired to establish the degree of electron trapping from representative fluences of fast neutrons in the $1MeV$ range.

A variety of sources for both neutron and charged particle irradiation are available and we propose to expose representative structures, such as a silicon drift detector with integrated electronics, and measure the several factors which will affect its SSC application:

1. Increase in leakage current from bulk generation through defects.
2. Decrease in collected charge caused by long term trapping.
3. Deterioration in time (position) measurement due to short term trapping.
4. Deterioration of the preamplifier performance.

In conclusion, it should be emphasized that there is really no data available that is applicable to describe the trapping of electrons moving in a drift field over long collection paths. Should trapping occur, carrier

removal is expected only to decrease collected charge (2 above) and not compromise the device as a tracking detector.

4.6 Complete read-out

Institutions: BNL, Harvard, Milano

A silicon drift detector based tracking system can provide, as mentioned earlier, space points with excellent spatial resolution from a relatively small number of electronic channels. For example with a drift distance of $1cm$ and typical interanode spacing of $200\mu m$ one needs only 50 channels per square centimeter. The effective pixel density for such a case is 2000 $pixels/cm^2$ if one further assumes $250\mu m$ double track resolution along the drift dimension. The price one pays for such a superb performance is in the level of sophistication of the readout electronics. Whereas a simple discriminator may be adequate for a silicon microstrip readout, careful time and charge measurements are required for a silicon drift detector. One typically employs dual shapers where each path is optimized for one or the other measurement. This solution, however, is not practical for a system with a large number of channels as the one we propose. A conventional flash ADC which could perform the function of both filters is also impractical for large systems. As is the case for most of the detectors for the SSC an analog pipeline would be necessary to buffer the data while the trigger decision is being made. Such a pipeline is a natural extension of the "built-in" pipeline provided by the drifting electrons. The characteristics of this pipeline are determined, in part, by the spatial extent of the drifting charge due to diffusion. For a typical drift field of $1kV/cm$ the diffusion length is $\approx 70 - 100\mu m$. With some charge integration (necessary for bandwidth limiting) the charge of a minimum ionizing particle is represented by a gaussian with a sigma of $\approx 150\mu m$. That implies that the bunch crossing frequency of the SSC is adequate as sampling frequency of the waveform. The dynamic range requirement for such a pipeline is a modest 8 bits.

Due to the enormous volume of data significantly more processing is required very close to the detector. We recognize the development of dedicated monolithic circuits as a major component of the required effort. We intend to address the following questions:

- How much processing "on-the-detector" is required;
- When to digitize;
- Feature extraction (cluster finding) in hardware;
- When/where to correlate drift times to resolve events from different bunch crossings;
- What technologies are suitable (radiation damage to electronics);
- What are the possibilities with ASICs especially ASICs with some built-in processing power.

Many of these problems are common to a lot of the proposed detectors for the SSC. We intend to follow closely related developments by other groups and perhaps collaborate with some in order to integrate into monolithic IC's many of these functions.

4.7 Fast trigger from silicon drift detectors

Institutions: Heidelberg, Milano

Silicon drift detectors provide the position information when the signal electrons arrive on the anode. For the SSC application it may be useful to have a prompt information to help to form a trigger. The prompt information may be obtained, in principle, from the signal induced by moving charges in the proximity of electrodes.

In a silicon drift detector the p^+ strips on both sides of the detector are normally used to provide the drift field for the generated electrons. They can also be used, once connected to preamplifiers (singularly or in groups), to get signals induced by electrons and holes. Electrons induce current signals of zero area because they are not collected by the p^+ strips. Holes produce, on those p^+ strips which collect them, a non zero area pulse.

These signal can be considered in order to obtain prompt information about charges generated and travelling in the detector within a time delay from the ionizing event much shorter than the total drift time of electrons through the whole length of the detector. Therefore, a suitable processing of these pulses, can lead to a useful trigger signal related for instance to the multiplicity evaluation of the tracks recorded by the detector.

Specific electrodes, in addition to the field electrodes, could be designed to get the most appropriate signals for triggering purposes.

The use of these prompt signals in silicon drift detectors has already been demonstrated for X-rays detection. The pulses were used as zero-time reference in the measurement of drift time for the determination of the position of interaction. Fig. 15 of [2] shows the diagram of electrode connections to obtain the zero–time reference from a silicon drift detector. Fig. 16 of the same reference shows the relevant waveforms at the output of the anode amplifier and at the output of the single amplifier connected to the p^+ strips.

For the trigger signal for the SSC application, one amplifier every 10 strips might be used. Let us call the required number of amplifiers n_a. The implementation of the additional n_a amplifiers allows to obtain the total charge released in the detector in $1/n_a$ of the total drift time.

4.8 Track and Vertex detector system

Institutions : All

This is the main scope of the proposal.

4.9 Monte Carlo

Institutions: Harvard, Princeton, Pittsburgh

We will start with same ISAJET simulation soon to avoid trivial mistakes. Heavy Monte Carlo study will start as soon as experimental numbers for the detector performance are known.

4.10 Spiraling tracks

Institutions: BNL, Milano

All silicon drift detectors in the proposed tracking system are placed perpendicular to the trajectories of fast particles produced at the interaction region. Thus their cross–section for low momentum spiraling tracks is smaller. The spiraling tracks cross the silicon drift detectors generally at a shallow angle leading to extensive ionization track. The cloud of electrons arriving to the anode from a hit by a spiraling particle has a very different shape that a cloud of electrons produced by a particle of normal incidence. We will attempt to analyze the pulse shape to suppress hits from spiraling tracks.

5. Milestones and Budget

5.1 Milestones

We hope to fulfill all tasks of the proposal in a 3 year period. Follow the list of important milestones.

1. 0.5 year. Test of the new version of the preamplifier on high resistivity silicon.
2. 0.5 year. Test of the NA45 silicon drift detector. This detector has a structure which does not allow electrons generated on the $Si - SiO_2$ interface to reach the detector anode.
3. 1 year. Radiation damage studies of the NA45 detector.
4. 1 year. Design of Mark1 SSC silicon drift detector.
5. 1.5 years. Production of Mark1 SSC silicon drift detector.
6. 2. years. Test of Mark1 SSC silicon drift detector.
7. 2. years. First radiation tests on Mark1.
8. 2. years. Design of the support and cooling structure for the track detector.
9. 2. years. Design of the read–out system.

10. 2.5 years. Completion of the tracker sector with Mark1 silicon drift detectors.
11. 2.5 years. Design of Mark2 SSC silicon drift detector.
12. 2.5 years. Test of the read–out system.
13. 3 years. Test of the complete sector.
14. 3 years. Monte Carlo studies.
15. 3 years. Production of Mark2 SSC silicon drift detector.
16. 3 years. Fast trigger from silicon drift detector.
17. 3 years. Spiraling track blind read–out system.

5.2 Budget

We are asking for the support of U.S. institutions only. Institutions in Italy will have their support from CNR, INFN and MPI; German institutions from BMFT and MPG. The only support from SSC fundings for the European collaborators would be contributions for masks and other production material.

We assume the same level of funding for the period of 3 years. Below are listed requirements for each U.S. institution per year.

Mask and production material		50 k
BNL	1 Full time mechanical engineer	80 k
	1 Full time electrical engineer	80 k
	2 Full time technicians (2 × 50 k)	100 k
	Equipment and material	60 k
	Travel	20 k
	TOTAL	340 k
Harvard	1 Full time electrical engineer	80 k
	1 Student	27 k
	Equipment	30 k
	Travel	10 k
	TOTAL	147 k
Princeton	1 Full time mechanical engineer	80 k
	1 Student	27 k
	Equipment	20 k
	Travel	8 k
	TOTAL	135 k
Pittsburgh	1 Full time electrical engineer	80 k
	1 Student	25 k
	Equipment and material	20 k
	Travel	10 k
	TOTAL	135 k
Rockefeller	1 Half time technician	25 k
	Equipment and Material	10 k
	Travel	3 k
	TOTAL	38 k
	GRAND TOTAL	845 k

6. References

1. E. Gatti and P. Rehak, Nucl. Instr. and Meth. 225, 608 (1984).
2. P. Rehak et al., Nucl. Instr. and Meth. A248, 367 (1986).
3. P. Rehak et al., IEEE Trans. on Nuclear Science,36, 203 (1989).
4. V. Radeka et al., IEEE Trans. on Nuclear Science, 35, 155 (1988).
5. V. Radeka et al., IEEE Electron Device Letters, 10, 91 (1989).
6. P. Rehak et al., to be published in Nucl. Instr. and Methods. and presented on the Fifth European Symposium on Semiconductor Detectors, Munich, March 1989.
7. H. Kraner et al., Nucl. Instr. and Methods, A279, 266 (1989)and SSC-SR-1035.
8. Coleman et al., Trans. on Nuclear Sciences, 15, 363 (1968).
9. Liu and Coleman, Trans. on Nuclear Sciences, 18, 192 (1971).